Speckle removal using a maximum-likelihood technique with isoline gray-level regularization

Nicolas Bertaux

Institut Fresnel, Equipe Φ-TI, Unité Mixte de Recherche 6133, Domaine Universitaire de Saint Jérôme, 13397 Marseille, France

Yann Frauel

Instituto de Investigaciones en Matemáticas Aplicadas y Sistemas, Universidad Nacional Autónoma de México, México, DF, Mexico

Philippe Réfrégier

Institut Fresnel, Equipe Φ-TI, Unité Mixte de Recherche 6133, Domaine Universitaire de Saint Jérôme, 13397 Marseille, France

Bahram Javidi

Department of Electrical and Computer Engineering, University of Connecticut, Storrs, Connecticut 06269-1157

Received February 10, 2004; revised manuscript received June 14, 2004; accepted July 19, 2004

We propose a method based on the maximum-likelihood technique for removing speckle patterns that plague coherent images. The proposed method is designed for images whose gray levels vary continuously in space. The image model is based on a lattice of nodes corresponding to vertices of triangles in which the gray level of each pixel is produced by linear interpolation. A constraint on isoline gray levels is introduced to regularize the solution. © 2004 Optical Society of America

OCIS codes: 100.0100, 100.3010, 030.0030, 030.4280.

1. INTRODUCTION

Many imaging systems use coherent light for illuminating the objects under study. This is the case for systems involving lasers and holography[1] as well as for synthetic aperture radar images.[2] Since they use coherent light, images obtained with these imaging systems are corrupted by speckle noise[3] that results from interference due to wave-front deformations. This speckle rapidly becomes an important drawback for further image processing. For example, a correlation between two identical images with different speckle patterns may provide a useless result, and speckle degrades most commonly used methods of detection or estimation.

Most of existing speckle-removing approaches are based on an image model with constant reflectivity in a patchwork of regions also known as a mosaic model. This image model is adapted for synthetic aperture radar images. For coherent optical images in general, the reflectivity of the objects in the scene can be continuously variable. This modification of the reflectivity can result, for example, from the three-dimensional structure of the objects.

In this paper we propose a new algorithm for speckle removal that is useful for image models that are more general than the mosaic one. The proposed method is based on the maximum-likelihood (ML) technique and uses a general model for image reflectivity. Moreover, to improve the quality of the result, a constraint on isoline gray level is imposed that allows one to obtain smooth results without blurring the edges of the objects in the image.

The structure of the paper is as follows. In Section 2 we describe the ML estimator according to speckle modelization. In Section 3 we introduce an image model defined as a continuous lattice based on elementary triangles. The algorithm designed for ML-criterion optimization is developed in Section 4. In Section 5 we introduce a regularization term based on the isogray level of the restored image. Validation and comparison with a classical method are provided in Section 6 before the conclusion in Section 7.

2. MAXIMUM-LIKELIHOOD ESTIMATOR

Active coherent imaging is useful for many applications. In particular, we consider in this paper the digital holography application. In fact, active coherent imaging allows one to implement digital holographic techniques in order to get three-dimensional information on the illuminated objects. In this case, a hologram is digitally recorded by a camera and then numerically processed to reconstruct arbitrary two-dimensional views of the three-dimensional object.[4,5]

The main difficulty with coherent imaging is the random high-spatial-frequency interference pattern (speckle), which in general cannot be perfectly predicted.

The complexity of radar or hologram scenes generally implies that the intensity level of the image must be regarded as a random field. The reflectivity of the scene, which is the parameter of interest, has then to be recovered from local parameters such as the local mean, the standard deviation, and the whole probability density function (pdf) of the random field.

Usually, intensity images with speckle correspond to the square modulus of Gaussian circular complex fields. Complex-field modelization could be obtained, for instance, from a wave front near the object calculated with digital holographic data.[4,5] For synthetic aperture radar images, one can get intensity images by averaging several independent intensity acquisitions. In that case, a simple but generally accurate speckle model for intensity images consists in considering that the gray levels are realizations of independent randoms fields with gamma pdf and that mean value is proportional to the local reflectivity in the image.

The pdf of the observed gray level x_n of pixel n is thus

$$p(x_n|i_n) = \left(\frac{L}{i_n^L}\right)\frac{x_n^{L-1}}{\Gamma(L)}\exp\left(-L\frac{x_n}{i_n}\right), \tag{1}$$

where i_n is the mathematical expectation value of the gray level at pixel n and L is the order of the gamma law. In this case, i_n corresponds to the gray level of the object that one would measure without speckle, and it is the information wanted. In the following, we will assume that L is known. Indeed, the pdf obtained with a complex Gaussian circular assumption on the amplitudes (which is the case of holography, for example) provides a gamma pdf for the intensity gray levels of order one ($L = 1$). Furthermore, averaging L images leads to gamma pdf of order L.

In the following, we will assume that the gray-level pixels of the image are distributed with gamma pdf [Eq. (1)] and that they are statistically independent. With this hypothesis, the log likelihood of the N pixel image $\mathbf{X} = \{x_n\}_{n\in[1,N]}$ can be written as

$$\ell(\mathbf{X}|\mathbf{I}) = \log\prod_{n=1}^{N} p(x_n|i_n), \tag{2}$$

where $\mathbf{I} = \{i_n\}_{n\in[1,N]}$ and which with Eq. (1) leads to

$$\ell(\mathbf{X}|\mathbf{I}) = C(L, \{x_n\}) - L\sum_{n=1}^{N}\left[\log(i_n) + \frac{x_n}{i_n}\right], \tag{3}$$

where $C(L, \{x_n\})$ is a term independent of $\mathbf{I}$.

The ML estimation of the intensity image $\mathbf{I} = \{i_n\}$ is obtained by maximizing the log likelihood[6] expression of Eq. (3):

$$\hat{\mathbf{I}} = \underset{\mathbf{I}}{\operatorname{argmax}}\,\ell(\mathbf{X}|\mathbf{I}). \tag{4}$$

One can remark that the ML estimation is independent of the L order of the gamma pdf. Indeed, the parameter L in Eq. (3) is present only in the additive constant $C(L, \{x_n\})$ and appears as the multiplicative factor of the second term that includes the parameter of interest $\mathbf{I}$.

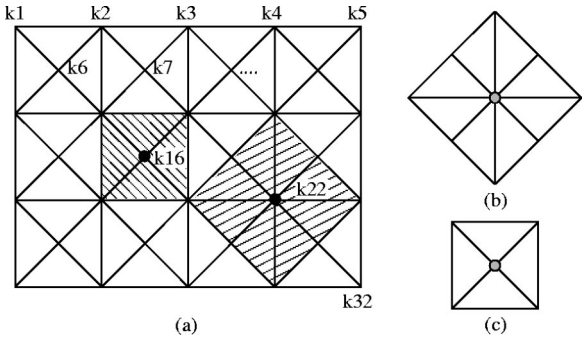

Fig. 1. Net example and its two base polygons.

3. IMAGE MODEL

Equation (3) shows that without further hypothesis, the ML estimator of the image $\mathbf{I}$ is the trivial result $\hat{\mathbf{I}} = \mathbf{X}$. Indeed, the first derivative of the log likelihood [Eq. (3)] with respect to i_n is

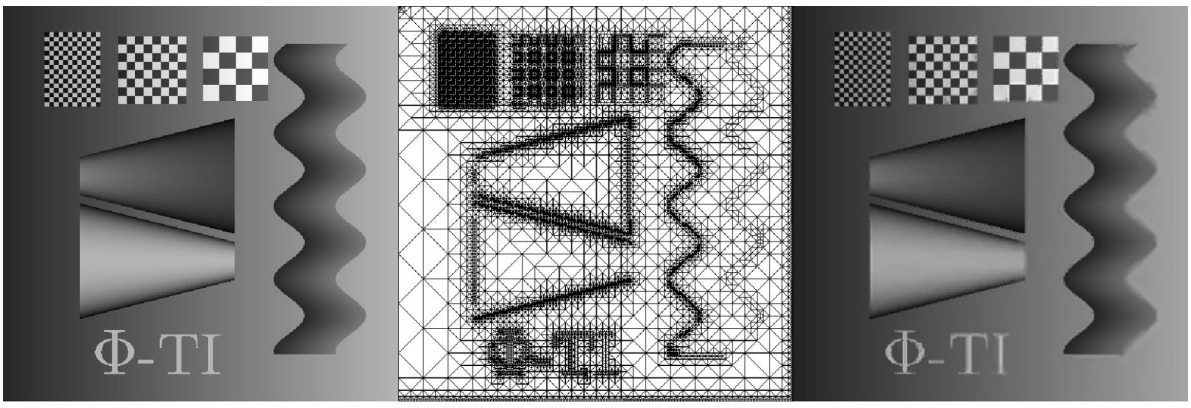

Fig. 2. An advantage of a lattice of triangles is adaptive complexity. (a) Reference image (513 × 513 pixels). (b) Example lattice with 11,369 nodes. (c) Modeled image using the lattice in (b).

$$\frac{\partial \ell}{\partial i_n} = \frac{1}{i_n} - \frac{x_n}{i_n^2} = \frac{i_n - x_n}{i_n^2}, \tag{5}$$

and this equation provides the solution:

$$\frac{\partial \ell}{\partial i_n} = 0 \Rightarrow i_n = x_n . \tag{6}$$

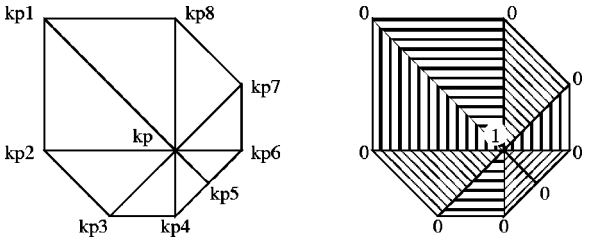

Fig. 3. Polygon-based elementary pyramid example used to compute the derivatives.

To remove speckle, one can limit the set of solutions of interest to images with slow spatial variations. An initial possibility consists in introducing an image model for **I**.

The choice of the image model is fundamental and must satisfy various contradictory constraints. The solution must remove the speckle by providing a smooth image. Furthermore, this solution should keep the edges between different objects. The last constraint that we consider is the computational time needed to find the solution. Let $\mathbf{K} = \{k_p\}_{p \in [1,P]}$ be a set of parameters that completely de-

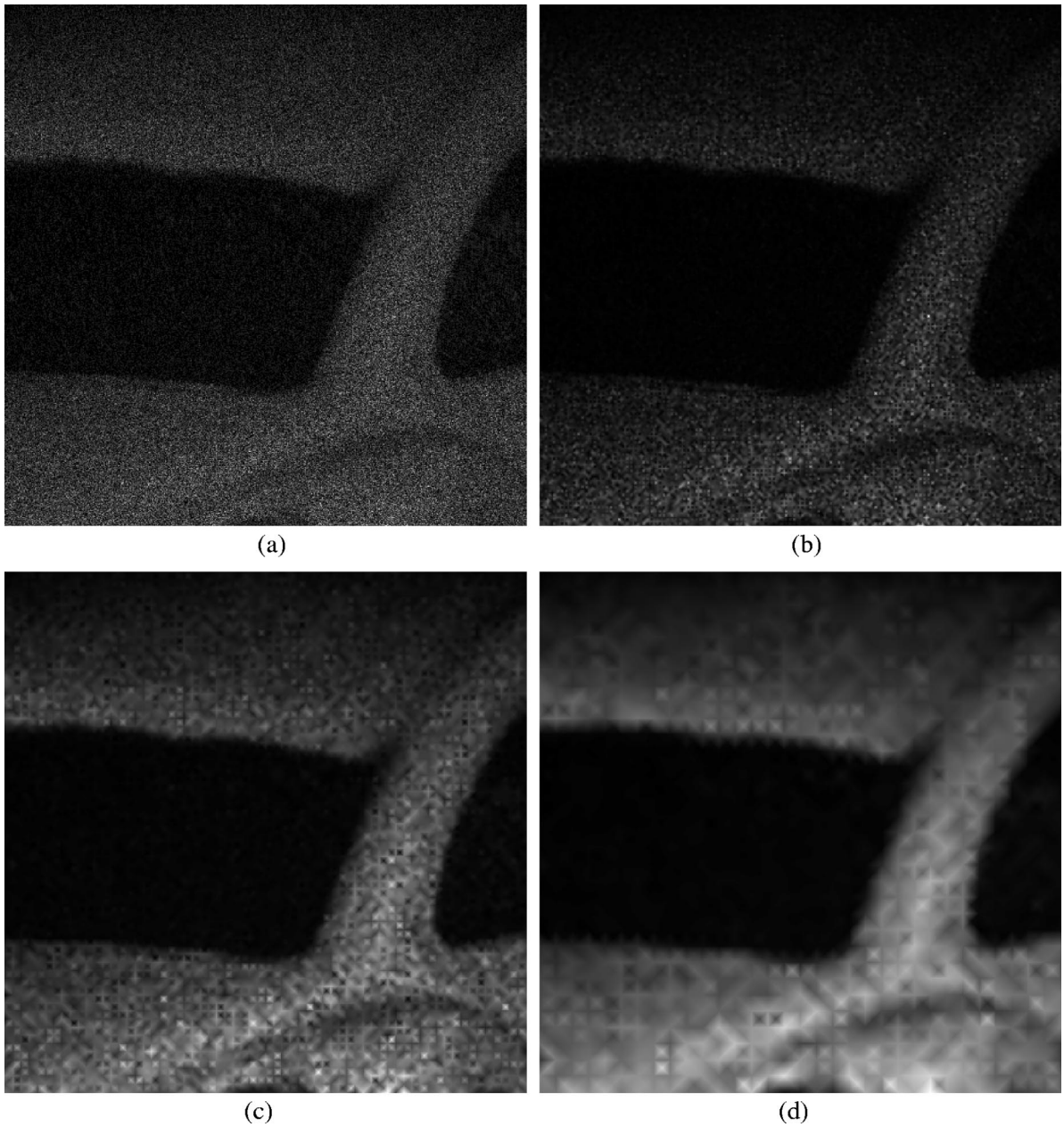

Fig. 4. Part of an image of a toy car calculated from an experimental digital hologram. Results are from different triangle sizes of the lattice. (a) Reference image 513 × 513, drawn with gamma correction = 2 only for visualization. (b) 5-pixel base triangle (1.5 s CPU time, 33,025 nodes). (c) 9-pixel base triangle (0.9 s CPU time, 8321 nodes). (d) 17-pixel base triangle (0.85 s CPU time, 2113 nodes).

fine the image $\mathbf{I}(\mathbf{K})$. P is the number of nodes in the lattice and thus is equal to the number of parameters of this model. The image model $\mathbf{I}(\mathbf{K})$ must be simple enough to lead to a low computational charge and must be dependent only locally on the parameters $\mathbf{K}$. In other words, when only one parameter k_p is modified, the image $\mathbf{I}(\mathbf{K})$ has to be modified on only a limited size area.

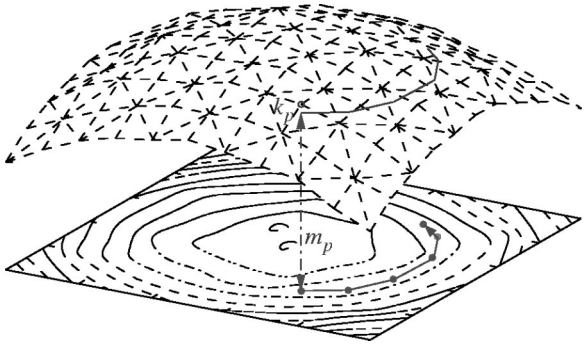

Fig. 5. Estimation of isoline level: description.

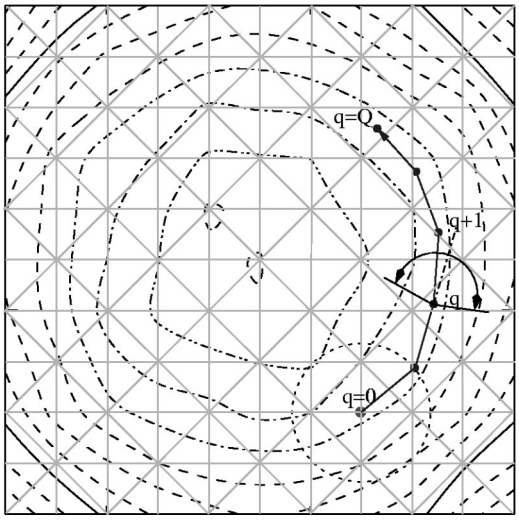

Fig. 6. Estimation of isoline level: determination.

We thus propose to consider a piecewise linear image model based on elementary triangles. Figure 1(a) shows an example of a lattice with two base polygons drawn separately in Figs. 1(b) and 1(c). The gray level of each pixel of the modeled image is defined as being a linear interpolation between the gray levels of three vertices of the triangle to which it belongs. This linear variation between nodes is a constraint that imposes a slow spatial variation of the intensity. Let each node k_p of the lattice be described by three coordinates $(k_{x_p}, k_{y_p}, k_{z_p})$, where k_{x_p}, k_{y_p} correspond to the coordinates of the node's location in the image and k_{z_p} is the unknown corresponding gray level. The parametric intensity image model can be written as

$$\mathbf{I} = \{i_n\} = \mathbf{I}(k_{z_1}, \ldots, k_{z_p}, \ldots, k_{z_P}). \tag{7}$$

The first advantage of using a simple lattice based on triangles is to lead to a low computational time. Indeed, determining the gray level for each pixel of the image from the triangle lattice information $(k_{z_1}, \ldots, k_{z_p})$ requires only $3N$ additions and $3N$ multiplications. This property is due mainly to the fact that local adjustments of the lattice result in local modifications of the gray level of the nearest pixels. Indeed, a modification of the gray level of one node implies computations only on the polygon area that surrounds this node. For example, the nodes k_{16} and k_{22} of the lattice shown in Fig. 1(a) are associated with polygons displayed, respectively, in Figs. 1(c) and 1(b).

The second advantage is the continuity of the gray level of the image model $\mathbf{I} = \{i_n\}$, which is introduced naturally by the lattice design. This continuity property is important for smoothing the image result.

The last advantage of the model is the ability of the lattice to be modified locally. Indeed, it is possible to add and remove nodes of the lattice without modifying the triangles that do not contain these nodes. The size of the

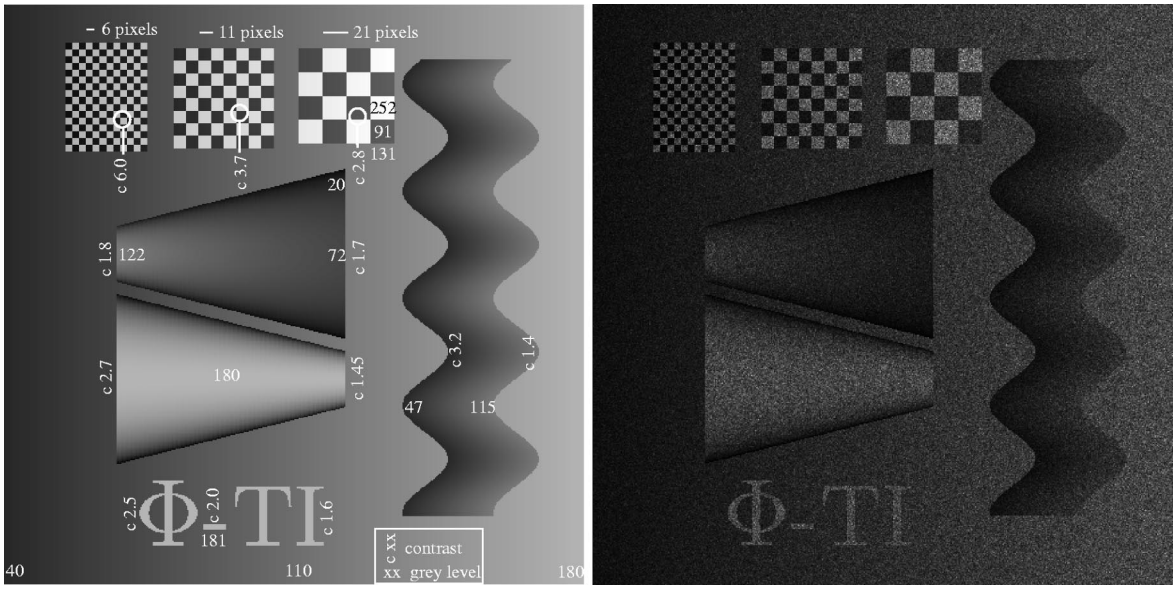

Fig. 7. Reference synthetic image and tenth-order gamma noisy image (512 × 512).

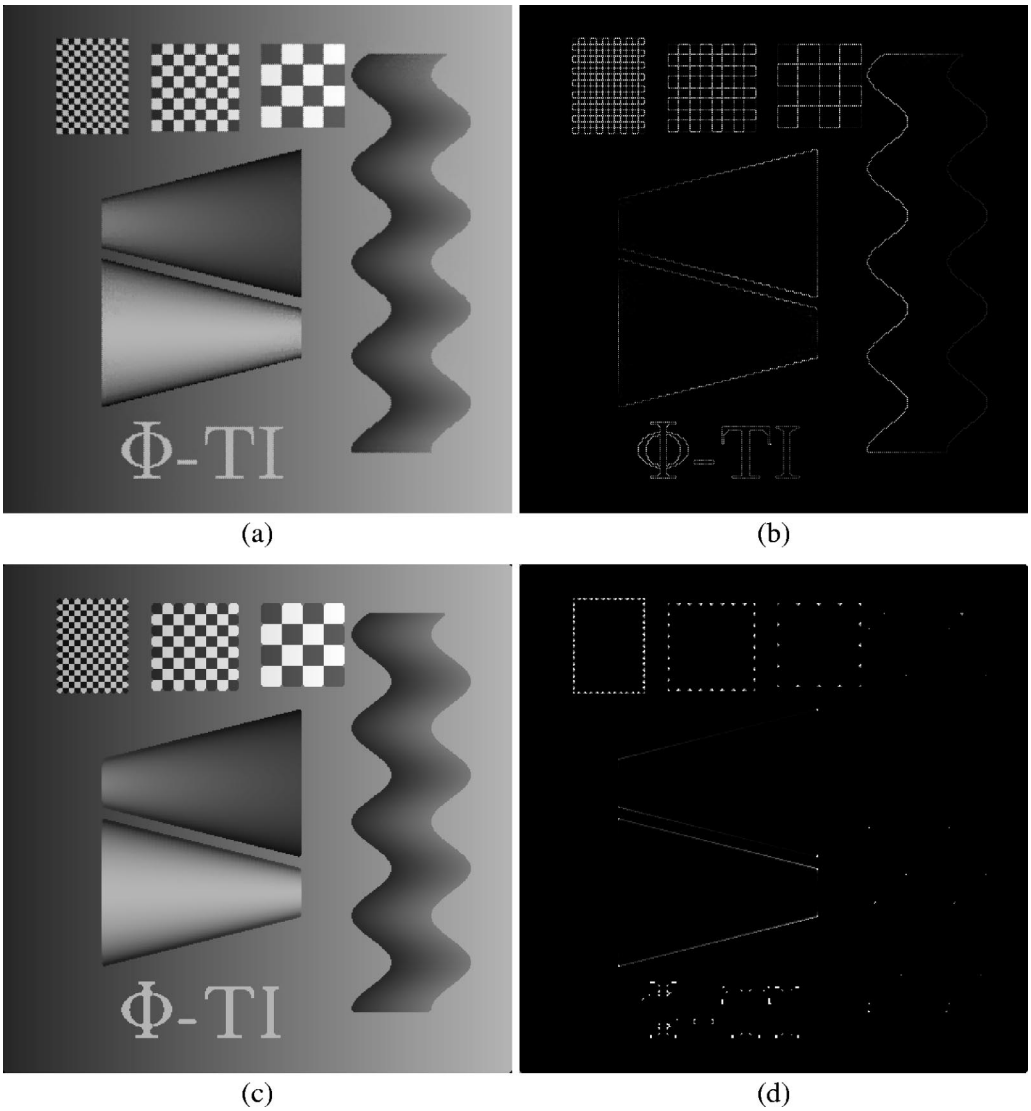

Fig. 8. Results for a synthetic image without noise (512 × 512). (a) $\mu = 0.15$ and $\beta = 0.14$ with 3-pixel base. (b) Square error image, mse = 100. (c) Median filter (5 × 5). (d) Square error image, mse = 44.

different triangles can therefore be adjusted to the image complexity: large triangles can be used for smooth surfaces and small triangles for details of the objects. A simple example is provided in Fig. 2, where Figs. 2(b) and 2(c) are examples of how the lattice can model the reference image Fig. 2(a). In this example, the lattice has 11,369 nodes for an image of size 513 × 513 pixels. In the following, a regular lattice will be used, but one can note that the proposed technique can be generalized to any lattice that is based on triangles.

4. OPTIMIZATION OF THE LOG-LIKELIHOOD CRITERION

To optimize the criterion at Eq. (3) with a low CPU load, a method with a small number of iterations has to be implemented. To determine the criterion for one 10^6-pixel image, close to 10^7 elementary computations are needed. We thus propose to implement an iterative second-order algorithm. Moreover, one can show that the triangular lattice with linear interpolation is very helpful for quick determination of the criterion derivatives. Indeed, the first derivative of the log-likelihood criterion with respect to the gray level k_{z_p} of the node k_p, is given by

$\forall\, k_p \in$ lattice

$$\frac{\partial \ell}{\partial k_{z_p}} = \sum_{n=1}^{N} \frac{\partial i_n}{\partial k_{z_p}} \frac{\partial \ell}{\partial i_n} = -L \sum_{n=1}^{N} \frac{\alpha_{p,n}}{i_n} \left(1 - \frac{x_n}{i_n}\right), \quad (8)$$

where $\alpha_{p,n} = \partial i_n / \partial k_{z_p}$. Actually, changes of k_{z_p} affect only the pixels contained in the polygons surrounding the node k_p, which will be denoted $\{p_1 \sim p_q\}$ (see Fig. 3). The value of $\alpha_{p,n}$ is zero for pixels outside this polygon. Equation (8) can thus be written as

$\forall\, k_p \in$ lattice:

$$\frac{\partial \ell}{\partial k_{z_p}} = -L \sum_{n \in \{p_1 \sim p_q\}} \frac{\alpha_{p,n}}{i_n} \left(1 - \frac{x_n}{i_n}\right). \quad (9)$$

Since the image model is defined by a linear interpolation between each two nodes of the lattice, then the set $\boldsymbol{\alpha}_p = \{\alpha_{p,n}/\text{pixel}\, n \in \{p_1 \sim p_q\}\}$ forms a pyramid with a po-

lygonal base $\{p_1 \sim p_q\}$—where the value is zero—and a top at node k_p—where the value is 1 (Fig. 3). This set of coefficients $\boldsymbol{\alpha}_p$ depends on the node k_p of the lattice. For the case of a regular lattice (presented in this paper), there are two different sets of coefficients according to the polygons Figs. 1(b) and 1(c).

With similar notation, the second derivative of the ML criterion can be written as

$\forall\, k_p \in$ lattice:

$$\frac{\partial^2 \ell}{\partial k_{z_p}^2} = -L \sum_{n \in \{p_1 \sim p_q\}} \frac{\alpha_{p,n}^2}{i_n^2} \left(2 \frac{x_n}{i_n} - 1 \right). \tag{10}$$

The second-order iterative algorithm that we propose to use to determine the k_{z_p} variation at each iteration can be written as

$$\forall\, k_p \in \text{lattice:} \qquad \Delta k_{z_p} = -\left(\frac{\partial^2 \ell}{\partial k_{z_p}^2} \right)^{-1} \frac{\partial \ell}{\partial k_{z_p}}. \tag{11}$$

Equation (11) provides z-axis correction for each node k_p. For a pixel n near a node k_p, the correction is $\Delta i_n = \Delta k_{z_p} \alpha_{p,n}$. The iterative process of the correction of the image model can thus be written as

$$\mathbf{I}_t = \mathbf{I}_{t-1} + \sum_{p=1}^{P} \Delta k_{z_p} \cdot \boldsymbol{\alpha}_p. \tag{12}$$

Owing to Eq. (12), $\mathbf{I}_t$ at iteration t is determined without extra computations, such as, for example, to reconstruct $\mathbf{I}_t$ from the set of values $\{k_{z_p}\}_{p \in [1,P]}$ known at iteration t. It is necessary only to determine at each iteration Δk_{z_p} with Eq. (11) and to modify the image model with Eq. (12).

5. REGULARIZATION WITH ISOLINE LEVEL

An initial regularization of the image $\{i_n\}$ is introduced naturally by the image model since it is based on a parametric model with fewer degrees of freedom than N, the

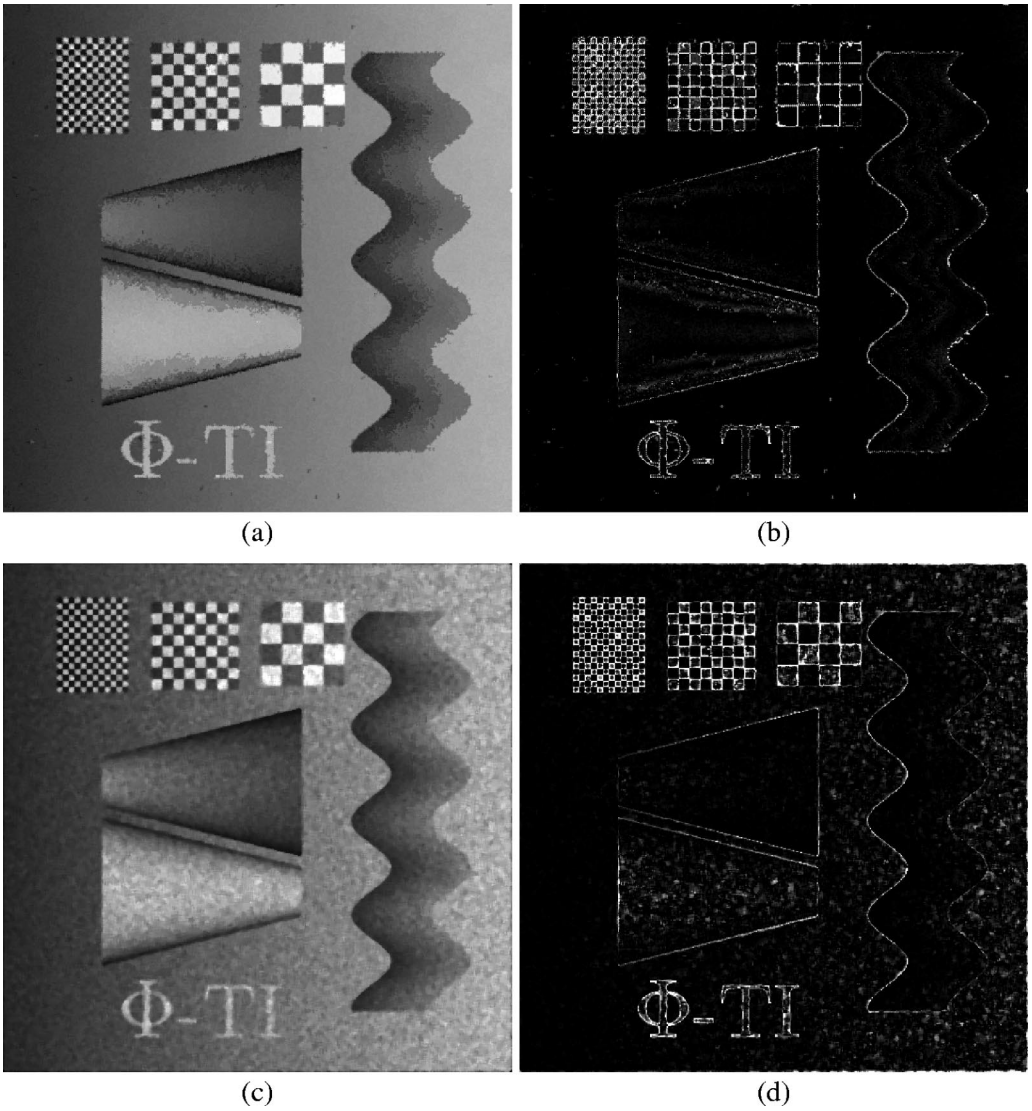

Fig. 9. Results for a synthetic image with tenth-order gamma noise (512 × 512). (a) $\mu = 0.15$ and $\beta = 0.14$ with 3-pixel base (46 s, PIII–1.1 GHz). (b) Square error image, mse = 219. (c) Median filter (5 × 5). (d) Square error image, mse = 362.

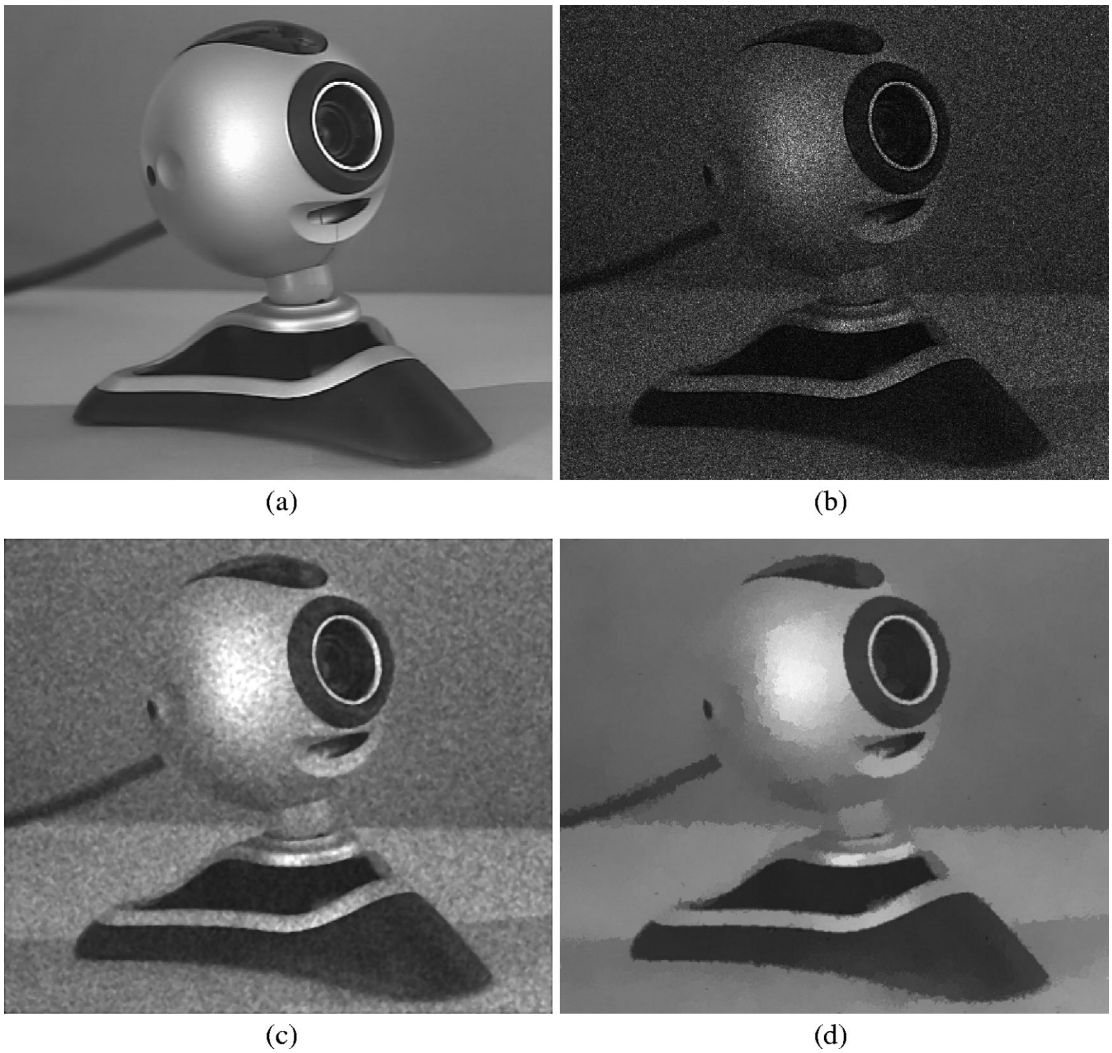

Fig. 10. Results on an optical CCD noisy image with 5th-order gamma noise (512 × 512 pixels). (a) Reference image (8 bits). (b) Noisy image perturbed by fifth-order speckle. (c) Mean filter (3 × 3) before the median filter (5 × 5), mse = 127. (d) Proposed technique with $\mu = 0.75$ and $\beta = 0.14$, mse = 73, 27 s.

pixel's image number. However, when small triangles are used, speckle noise removal is unsatisfactory, as shown in Fig. 4. This figure, a part of a toy car, is a reconstructed two-dimensional view next to an experimental digital hologram with 12-bit dynamic range. Figure 4(a) shows the initial image without speckle removal. Figures 4(b), 4(c), and 4(d) show the results obtained for different sizes of the elementary triangle. One can see that noise removal is very poor with triangles that have a base of 5 pixels. In Fig. 4(c) the base of the triangle was 9 pixels, and noise removal is still quite poor. On the other hand, with triangles that have a 17-pixel base, the speckle noise has been more efficiently removed, but a blurring effect becomes noticeable and prohibits the use of larger-triangle modelization.

To improve speckle removal, we propose to introduce, with small triangles, a second constraint. This constraint brings minimal *a priori* information on the smoothness of the result.

Since most common images are continuous images with a small number of edges, images can be decomposed into regular lines with constant gray levels (Fig. 5). Furthermore, these iso-gray-level lines (which will be simply denoted isolines in the following) are in general regular in the sense that their shape does not oscillate much. The principle of the proposed isoline regularization thus consists in penalizing irregular sets of constant gray levels. More precisely, starting from one node k_p of coordinates (k_{x_p}, k_{y_p}) of the triangle lattice, one looks for pixel l_1 in a circle of radius equal to the size of the base of the triangles centered on the node k_p that has a gray level nearest to k_{z_p}. Let us assume that an isoline has been determined with $q - 1$ pixels. To merge a new pixel l_q to this isoline, a half-circle of radius equal to the size of the base of the triangles is first defined in the direction $l_{q-2}\overrightarrow{l_{q-1}}$ as shown in Fig. 6. Let $i_{l_1},\ldots,i_{l_{q-1}}$ denote the gray-level values of the pixel $l_1,\ldots,l_{q-1}$ of the isoline with $q - 1$ pixels. One can thus define the mean gray-level value of this isoline $m_{q-1} = \frac{1}{q-1}\Sigma_{j=0}^{q-1} i_{l_j}$, where l_0 corresponds to k_p. One thus has to determine in the half-circle defined above the pixel l_q that has a gray level value i_{l_q} the nearest to m_{q-1}. If $|i_{l_q} - m_{q-1}|/m_{q-1}$ is smaller than a threshold β (denoted "constrast threshold"), the pixel l_q is

merged with the isoline and the process is iterated. The merging process is stopped when this condition can no longer be fulfilled or when the maximum length of the isoline level, fixed at the beginning, has been reached. A new merging process is then initiated with another node of the lattice.

Since this process is applied on the restored image obtained at iteration t, the proposed technique thus consists in minimizing,

$$J(\mathbf{I}(\mathbf{K})) = C + L \cdot \sum_{n=1}^{N} \left\{ \log[i_n(\mathbf{K})] + \frac{x_n}{i_n(\mathbf{K})} \right\} + \mu \cdot L \cdot \sum_{p=1}^{P} N_p \frac{[k_{z_p} - m_p(\beta)]^2}{m_p(\beta)}, \quad (13)$$

where μ is a parameter that balances the likelihood term (first part of the criterion) and the regularization one, N_p is the number of pixels that belong to the polygon $\{p_1 \sim p_q\}$ that includes the node k_p, β is the parameter of the regularization method, and P is the number of nodes in the lattice. As shown in Eq. (13) the proposed technique consists in determining the isoline m_p to which each node belongs in order to penalize the square difference between the gray level of nodes and their corresponding isolines. In addition, the square difference in node p is weighted by the isoline gray-level value L/m_p in order to take into account the characteristics of speckle noise, which is a multiplicative noise.

6. VALIDATION AND COMPARISON OF SYNTHETIC AND REAL IMAGES

Many methods have been proposed to remove speckle, but few lead to a fast algorithm. Furthermore, it is not possible to compare the proposed technique with all of them, and we will restrict our analysis to the most common and rapid technique. We will thus compare in this section the proposed method with a classical median filtering technique.

The synthetic image used for the tests is shown in Fig. 7. This image presents borders with strong slopes of one pixel and continuous variations of gray levels. Some gray-level values are presented in Fig. 7(a) (horizontal text), and the contrasts for some borders are also reported (vertical text). Figure 7(b) shows the noisy image generated with a tenth-order speckle noise with a gamma pdf defined by Eq. (1).

To analyze the efficiency of the considered speckle-removing techniques, we propose to analyze the effect of the techniques on an image without noise. Figures 8(a) and 8(b) show these results: One can observe in Fig. 8(b) the square error that is due to the triangular lattice modelization. The mean square error (mse) on the image is 100. Figures 8(c) and 8(d) show the result for a 5×5 median filter. Figure 8(d) shows the error introduced by the sliding window processing. It is important to note that the mse (44) of the median filter is lower than that for the one of the proposed techniques (100).

Figure 9 shows the results for the gamma noisy synthetic images. The results of the proposed technique are shown in Figs. 9(a) and 9(b) and were obtained by use of a triangle lattice with a 3-pixel base and with regularization by isoline level. Figures 9(c) and 9(d) show the results of median filtering technique (with a sliding window of 5×5 pixels).

Results shown in Fig. 9(a) demonstrate that the proposed method is able to remove speckle efficiently while keeping sharp edges between the different zones. Of course, estimation of the edges is not perfect for low contrasts; however, we can conclude from Fig. 9(a) that the

Fig. 11. Top, reference image of a toy car reconstructed from an experimental digital hologram of 1123×1585 pixels with first-order speckle (or one look), drawn with modification of gray levels for visualization. Middle, result with 3-pixel base triangle, $\mu = 5.0$ and $\beta = 0.3$ (260 s, 889,978 nodes, PIII–1.1 GHz). Bottom, result with 5-pixel base triangle, $\mu = 5.0$ and $\beta = 0.3$ (61 s, 222,437 nodes, PIII–1.1 GHz).

contrast limit for obtaining good results is between 1.1 and 1.2 for tenth-order speckle. For high-contrast edges, one can observe from Fig. 9(b) that the quality of the restoration is limited by the size of the lattice. More precisely, the resolution of the restored image is roughly determined by the size of the triangles of the lattice. In addition, and in contrast to the results of the median filter shown in Figs. 9(c) and 9(d), the restoration of the gray levels of the surfaces is very smooth, and its quality is visually the same for any mean value of the gray level. The mse is 219 for the restoration provided by the proposed technique and 362 for the median filter.

The next validation is based on a real image of the camera (8-bit dynamic) shown by Fig. 10(a), which is perturbed by fifth-order speckle noise as shown in Fig. 10(b). Figure 10(d) shows the restored image produced with the proposed technique with a 3-pixel base triangle. The restored image produced by a median filter is shown in Fig. 10(c). For this low-order speckle, the image of Fig. 10(c) was obtained by first applying a low-pass filter of size 3×3 pixels with all filter coefficients equal to 1/9 and then a 5×5 median filter. The mse is 73 for the proposed technique [Fig. 10(d)] and 127 for the median filter [Fig. 10(c)]. One can also see that with the proposed technique the visual aspect is improved in comparison with the result obtained with a median filter.

The last validation is based on the reconstructed two-dimensional view of an experimental digital hologram where the speckle corresponds to first-order speckle. Figure 11 presents the result for a lattice with 3 and 5 pixels for the base of the triangles and a constraint on the isoline level.

7. CONCLUSIONS AND PERSPECTIVES

Using the hypothesis of a gamma pdf of the speckle, we provided a maximum-likelihood estimator of the reflectivity of the object. An initial regularization was introduced in the form of a lattice modelization. This model allows one to obtain an efficient algorithm from a computation point of view. We proposed a further improvement of the technique by introducing an efficient regularization by isoline level. The latter technique keeps the edges of the objects while providing smooth surfaces.

The principal perspective of this work is to generalize it to an autoadaptive lattice, where it will not be necessary to use a constraint on the isoline level.

Corresponding author Nicolas Bertaux can be reached at the address on the title page or by e-mail: nicolas.bertaux@fresnel.fr.

REFERENCES

1. H. J. Caulfield, *Handbook of Optical Holography* (Academic, London, 1979).
2. C. Oliver and S. Quegan, *Understanding Synthetic Aperture Radar Images* (Artech House, Boston, Mass., 1998).
3. M. Françon, *Laser Speckle and Application in Optics* (Academic, New York, 1979).
4. U. Schnars and W. P. O. Jüptner, "Direct recording of holograms by a CCD target and numerical reconstruction," Appl. Opt. **33**, 179–181 (1994).
5. Y. Frauel, E. Tajahuerce, M.-A. Castro, and B. Javidi, "Distortion-tolerant three-dimensional object recognition with digital holography," Appl. Opt. **40**, 3887–3893 (2001).
6. H. L. Van Trees, *Detection Estimation and Modulation Theory* (Wiley, New York, 1968).